Osteoblasts are inherently programmed to repel sensory innervation

L. Leitão[1,2,3], F. Conceição[1,2,3], E. Neto[1,2], A.C. Monteiro[1,2], M. Couto[1,2,3], C.J. Alves[1,2], D. Sousa[1,2] and M. Lamghari[1,2]

[1]i3S – Instituto de Investigação e Inovação em Saúde, Universidade do Porto – Associação; [2]INEB – Instituto de Engenharia Biomédica; [3]ICBAS – Instituto de Ciências Biomédicas Abel Salazar.

Francisco Conceição
francisco.conceicao@ineb.up.pt

Estrela Neto
estrela.neto@ineb.up.pt

Meriem Lamghari
lamghari@ineb.up.pt

Background

Tissue innervation is a complex process controlled by the expression profile of signaling molecules secreted by tissue-resident cells that dictate the growth and guidance of axons. Sensory innervation is part of the neuronal network of the bone tissue with a defined spatiotemporal occurrence during bone development. Yet, the current understanding of the mechanisms regulating the map of sensory innervation in the bone tissue is still limited. An accurate picture of this crosstalk is of the utmost importance and will, ultimately, allow researchers and clinicians to unravel new candidates as potential targets, not only for bone pain therapies, but also to control the neuropathological outcomes resulting from the disturbances in bone cell activity.

Results

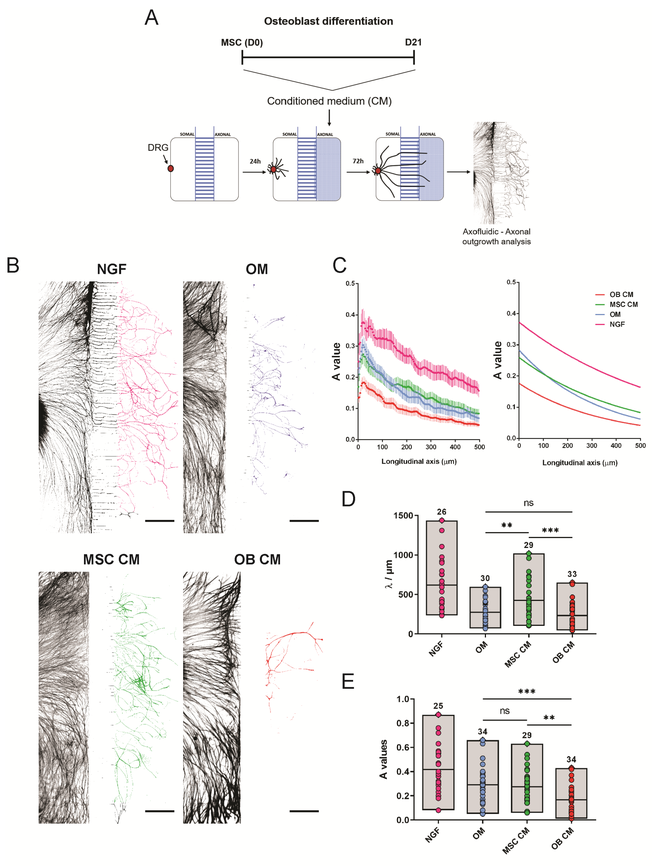

Figure 1: The secretome of mature OB applied locally to sensory axons, alters their behavior, and impairs their growth. **a** Scheme of the experimental setup and timeline employed in these experiments. **b** Representative images used for the quantification of the axonal growth upon 72 h exposure to standard neuronal growth medium containing NGF (positive control), osteogenic medium (OM), undifferentiated (MSC CM), and mature osteoblasts (OB CM) conditioned medium (axons stained against βIII-tubulin; scale bar—500 μm). **c** The combined plot of the data obtained using Axofluidic from all of the quantified microfluidic devices in the different conditions (left), and corresponding graphical representation of the exponential model (right), described by the spatial dependence decay function that best fits the data. A value represents the amount of axons that cross the microgrooves and reach the axonal side, whereas in the longitudinal axis is represented the distance from the microgrooves (in μm). **d, e** Graphical representation of all A values (c) and λ values (d) in the different conditions. Results are presented as floating bar graphs (line represents the mean value, and the number above each bar represents the number of microfluidic devices that were analyzed; **P < 0.01; ***P < 0.001, ns non-significant).

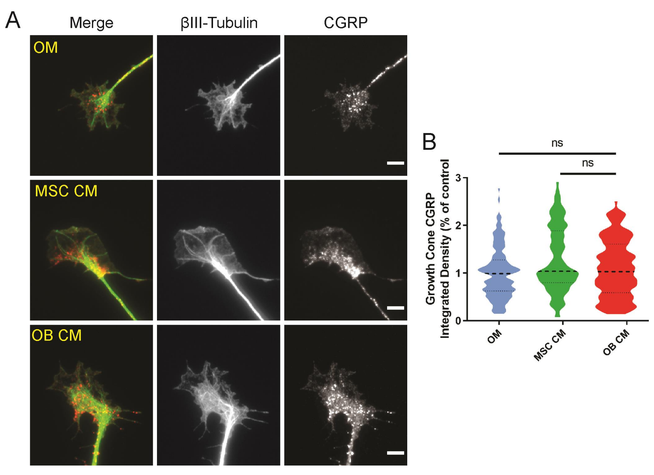

Figure 2: The secretome of OB-lineage cells does not impact the expression of CGRP at the growth cones of sensory neurons. **a** Representative images of the sensory growth cones exposed to osteogenic medium (OM), undifferentiated (MSC CM), and mature osteoblasts (OB CM) conditioned medium for 72 h (green—βIII-tubulin; red—CGRP; scale bar—5 μm). **b** Graphical representation of the integrated intensity of CGRP in different conditions. Results are presented as violin plot (middle dashed line represents the median value; upper and lower dashed lines represent the quartiles; ns non-significant

Conclusions

- differentiation of human mesenchymal stem cells to osteoblasts leads to a marked impairment of their ability to promote axonal growth;
- mechanisms include paracrine-induced repulsion and loss of neurotrophic factors expression;
- reduction of NGF and BDNF production and stimulation of Sema3A, Wnt4, and Shh expression culminating at late stage of OB differentiation.
- blockade of Shh activity and signaling reversed the repulsive action of osteoblasts on sensory axons.

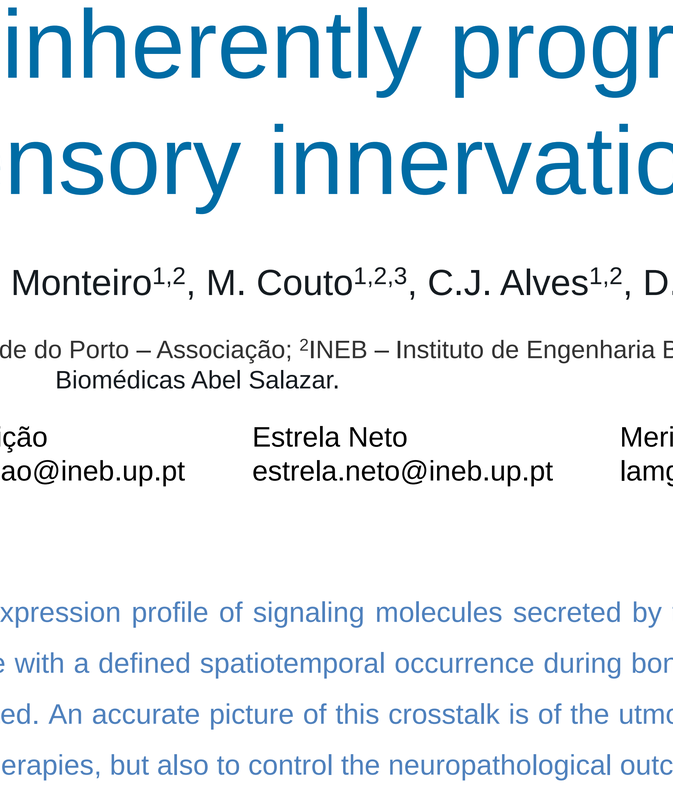

Figure 3: Mature OB prevent the growth of sensory axons in a coculture setup in compartmentalized microfluidic devices. **a** Coculture of DRG with OB-lineage cells at different time points of differentiation, i.e., undifferentiated MSC (top left), with 7 (top right), 14 (bottom left), and 21 (bottom right) days of differentiation (green—F-Actin; red—βIII-tubulin; blue—DAPI; scale bar—500 μm). Of notice, the progressive reduction in the number of axons in the OB-lineage cell compartment throughout OB differentiation. For better visualization of the axons present in the axonal compartment, a region was selected (dashed blue line) showing only the axons (red—βIII-tubulin; scale bar—200 μm). **b** Sensory axons growing and contacting undifferentiated MSC (white arrow, scale bar—25 μm). **c** Axons (white arrow) entering the microgrooves of the microfluidic device without reaching the OB compartment in the coculture setting of DRG and OB with 21 days of differentiation (dashed lines represent the microgrooves. Scale bar—25 μm).

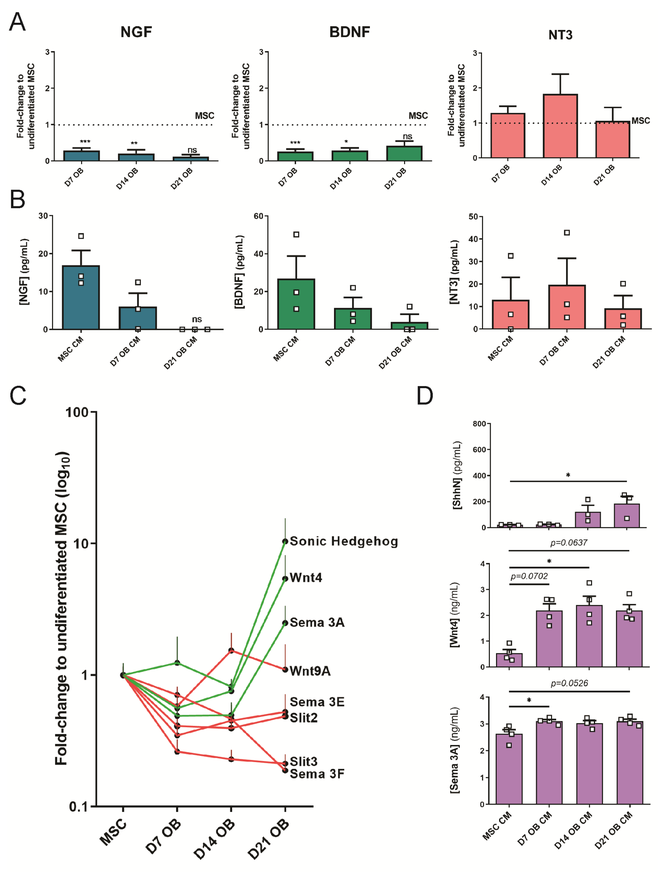

Figure 4: OB differentiation downregulates the expression of neurotrophic factors and upregulates the expression of axonal repulsive cues. **a** Gene expression analysis of NGF, BDNF, and NT-3. Values normalized to the values of undifferentiated MSC (horizontal dashed line). **b** ELISA analysis of NGF, BDNF, and NT-3 in the conditioned medium of OB at different stages of differentiation. **c** Fold-change variation in the gene expression of the selected axonal repulsive cues throughout OB differentiation. Values normalized to the values of undifferentiated MSC. Red lines depict the proteins that downregulated or showed no significant changes. Green lines depict the proteins that upregulated. **d** ELISA analysis of Shh, Sema3A, and Wnt4 in the conditioned medium of OB at different stages of differentiation. *P < 0.05; **P < 0.01; ***P < 0.001

Citation: L. Leitão, E. Neto, F. Conceição, A. Monteiro, M. Couto, C.J. Alves, D.M. Sousa, M. Lamghari, Osteoblasts are inherently programmed to repel sensory innervation, Bone Res. 8 (2020) 20; Funding: FEDER—Fundo Europeu de Desenvolvimento Regional funds through the COMPETE 2020—Operacional Programme for Competitiveness and Internationalisation (POCI), Portugal 2020, and by Portuguese funds through FCT/ MCTES in the framework of the project SproutOC (PTDC/MED-PAT/30158/ 2017; POCI-01-0145-FEDER-030158).

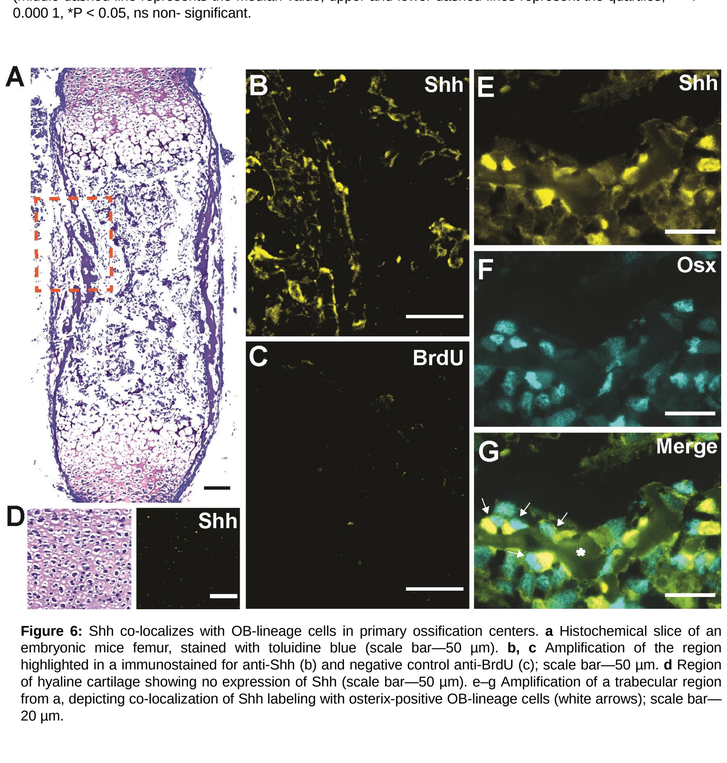

Figure 5: OB-derived Shh contributes to sensory axonal repulsion. **a** Scheme of the experimental setup and timeline employed in these experiments. **b, c** Graphical representation of A values (a) and λ values (b) for OB CM alone or supplemented with the Shh activity blocker antibody 5E1, the isotype control antibody anti-BrdU (G3G4), the Smo antagonist SANT-1, and the positive control Shh diluted in OM. Results are presented as floating bar graphs (line represents the mean value, and the number above each bar represents the number of microfluidic devices that were analyzed; **P < 0.01; ns non-significant). **d** Representative images of the sensory growth cones exposed for 10 min to mature osteoblasts (OB CM) alone, and supplemented with the 5E1 and G3G4 antibodies (green—GAP-43; red—phosphorylated PKCα; scale bar— 5 μm). **e** Graphical representation of the integrated intensity of phosphorylated PKCα in different conditions. Results are presented as violin plot (middle dashed line represents the median value; upper and lower dashed lines represent the quartiles; ****P < 0.000 1, *P < 0.05, ns non- significant.

Figure 6: Shh co-localizes with OB-lineage cells in primary ossification centers. **a** Histochemical slice of an embryonic mice femur, stained with toluidine blue (scale bar—50 μm). **b, c** Amplification of the region highlighted in a immunostained for anti-Shh (b) and negative control anti-BrdU (c); scale bar—50 μm. **d** Region of hyaline cartilage showing no expression of Shh (scale bar—50 μm). e–g Amplification of a trabecular region from a, depicting co-localization of Shh labeling with osterix-positive OB-lineage cells (white arrows); scale bar—20 μm.

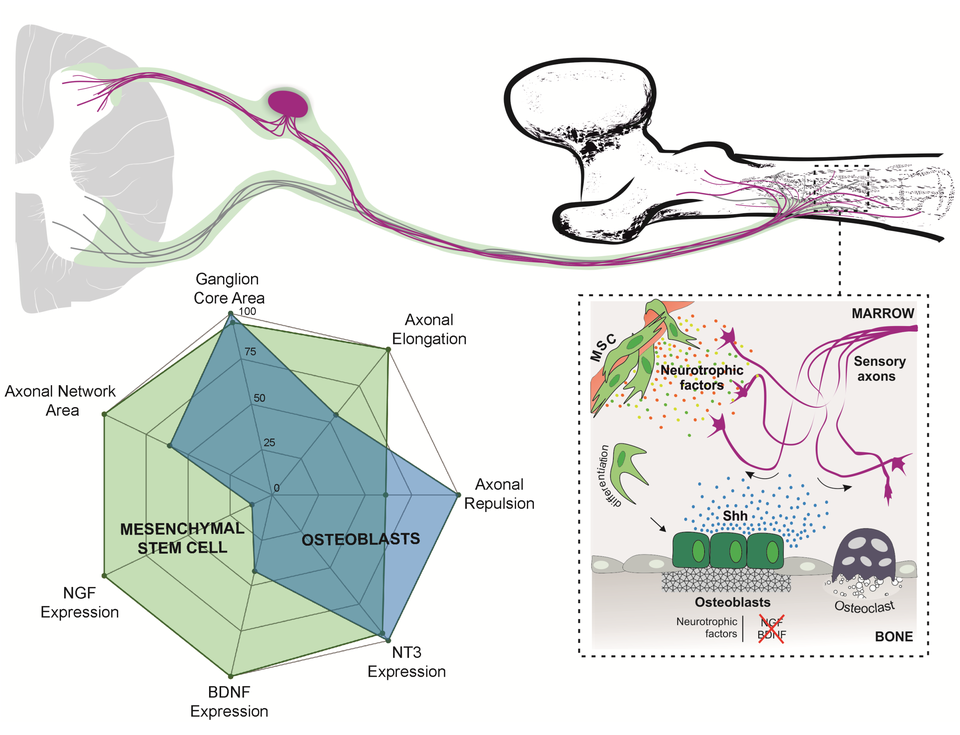

Figure 7: Overall model summarizing the remarkable ability mature OB have to repel and impair the growth of sensory axons.